

Ultrasound propagation in bond frustrated HgCr_2S_4 spinel in magnetic fields

V. Felea¹, L. Prodan¹, E. Stefanet¹, P.T. Cong², S. Zherlitsyn², and V. Tsurkan^{1,3}

¹*Institute of Applied Physics, Academy of Sciences of Moldova, MD-2028, Chişinău, R. Moldova*

²*Hochfeld-Magnetlabor Dresden (HLD-EMFL), Helmholtz-Zentrum Dresden-Rossendorf, D-01314 Dresden, Germany*

³*Experimental Physics V, Center for Electronic Correlations and Magnetism, Institute of Physics,
University of Augsburg, D 86159 Augsburg, Germany*

E-mail: vtsurkan@yahoo.co.uk

Received October 17, 2016, published online March 24, 2017

Ultrasound and magnetization studies of bond frustrated spinel HgCr_2S_4 are performed as a function of temperature in static magnetic fields. Beside the anharmonic effect, the sound velocity shows pronounced anomaly at the antiferromagnetic (AFM) transition at $T_N = 23$ K with an additional significant increase of the order of 0.5% indicating a strong spin-lattice coupling. External magnetic fields enhance the ferromagnetic (FM) correlations and shift the anomalies to lower temperatures concomitantly with the reduction of the Néel temperature. The constructed H - T phase diagram beside the long-range AFM states reveals the state with induced FM order and regimes with short-range AFM and FM correlations as well.

PACS: **43.35.+d** Ultrasonics, quantum acoustics, and physical effects of sound;
62.65.+k Acoustical properties of solids;
72.55.+s Magnetoacoustic effects;
75.50.Ee Antiferromagnetics;
75.60.Jk Magnetization reversal mechanisms.

Keywords: geometrical frustration, H - T phase diagram, spinel, magnetization.

Ternary chromium oxide and chalcogenide spinels with the formula ACr_2X_4 have been intensively studied in last decades. They manifest unusual phenomena and exotic ground states including complex spin degrees of freedom, relaxor multiferroicity and colossal magnetoresistance [1–6]. Strong competition of antiferromagnetic (AFM) and ferromagnetic (FM) interactions and geometrical frustration [7] establish a fascinating phase diagram of ACr_2X_4 spinels with complex magnetic ground states [8]. The magnetism in chromium oxide spinels is governed by a strong nearest neighbor Cr–Cr AFM exchange within the corner-sharing tetrahedral network of the magnetic ions, a prototypical example of a geometrically frustrated pyrochlore lattice. The oxide spinels undergo an antiferromagnetic spin order transition at temperatures T_N much lower than the Curie–Weiss temperature Θ_{CW} characterizing the strength of the dominating exchange. The magnetic transitions in the chromium oxide spinels are frequently accompanied by structural distortions which have been interpreted in terms of a spin-driven Jahn–Teller (JT) effect [9,10]. In sulfide and selenide

spinel the direct Cr–Cr exchange is less effective and the indirect Cr–X–Cr exchange becomes more important leading to a competition of the AFM and FM interactions, or bond frustration. In the chromium sulfide and selenide spinels, ZnCr_2S_4 and ZnCr_2Se_4 , the observed splitting of the phonon modes on entering into the antiferromagnetic state [11,12] was attributed to a strong spin-lattice coupling. In these materials the Cr^{3+} ions in the octahedral crystal field reveal a nearly spherical charge distribution with the g factor close to 2 [13]. Significant spin-phonon coupling was also found in CdCr_2S_4 ferromagnet and in HgCr_2S_4 metamagnet with the AFM ground state. These two sulfide compounds are dominated by the strong ferromagnetic exchange. Although no splitting of the phonon modes was detected at the magnetic phase transitions in CdCr_2S_4 and HgCr_2S_4 , IR spectroscopy studies documented significant effects in the temperature dependences of the plasma frequencies indicating changes of the nature of the bonds and charge transfer [14]. Moreover, the specific polar modes in HgCr_2S_4 reveal the shifts exactly correlated with the magnetic-field-

dependent magnetization indicating strong magnetodielectric effect [14]. In a view of colossal magnetocapacitance and relaxor multiferroicity observed in CdCr_2S_4 and HgCr_2S_4 [4,15] this underlines the importance of the spin-lattice coupling in understanding the nature of the multiferroic behavior of the chromium sulfide spinels. Multiferroic materials with concurrent magnetic and ferroelectric orders are the subject of intensive current theoretical and experimental investigations. These interesting materials not only challenge the understanding of the ordering phenomena in solids but also provide new functionalities in spintronics since the dielectric and magnetic polarizations can be tuned by either external magnetic or electric fields [16–19].

In this paper we present the results of the experimental study of sound propagation in HgCr_2S_4 spinel aimed to provide further insight into magnetoelastic coupling of this compound. The ultrasound technique is known as a powerful tool for study of the magnetoelastic properties of solids being extremely sensitive to structural and magnetic changes [20].

The material under the study, HgCr_2S_4 , crystallizes in a normal cubic ($Fd\bar{3}m$) spinel structure with diamagnetic Hg^{2+} ions occupying the tetrahedral A sites and magnetic chromium ions (Cr^{3+} , $3d^3$ with $S = 3/2$) occupying the octahedral B sites. At low temperature this compound develops a long-range AFM spin order in spite of high positive Curie–Weiss temperature $\Theta_{CW} = +142$ K that indicates the dominance of strong FM exchange at high temperatures [21]. Earlier neutron-diffraction investigations at low temperatures and in zero magnetic field revealed a spiral spin configuration [22] suggesting that HgCr_2S_4 is an antiferromagnet below a critical temperature of 60 K. A similar conclusion was provided by the optical studies [23]. Further detailed analysis of the properties of HgCr_2S_4 by magnetization, electron-spin resonance, and specific-heat documented the appearance of strong ferromagnetic fluctuations below 50 K and the occurrence of a complex long-range antiferromagnetic order only below $T_N = 22$ K [24]. A highly unconventional behavior was observed, which resembles properties of a noncollinear antiferromagnet and of a soft ferromagnet depending on temperature and magnetic field. It was shown that even weak external magnetic fields disturb the antiferromagnetic order and strongly enhance the ferromagnetic correlations. Further high-resolution powder neutron diffraction investigations [25] established that the long-range incommensurate magnetic order with propagation vector $(0,0,\sim 0.18)$ sets in at $T_N \sim 22$ K, in agreement with the results of the studies of the macroscopic properties in [24]. On cooling below T_N , the propagation vector increases and saturates at the commensurate value $(0,0,0.25)$. The magnetic structure below T_N consists of ferromagnetic layers in the ab plane stacked in a spiral arrangement along the c axis. The symmetry analysis performed in [25] revealed a point group symmetry in the ordered magnetic phase of 422 (D_4) which is incompatible

with the macroscopic ferroelectricity, indicating that the spontaneous dielectric polarization observed experimentally in [15] cannot be coupled to the magnetic order parameter.

We have performed the ultrasound propagation and magnetic measurements of single crystalline HgCr_2S_4 spinel aimed to study magnetoelastic coupling and to deduce the thermodynamic H – T phase diagram.

The single crystals of HgCr_2S_4 have been grown by the chemical transport reaction method using the ternary polycrystalline material prepared by solid-state reactions and chlorine as the transport agent. The growth experiments were performed at temperatures between 850 and 900 °C. Structural analysis of the grown crystals was performed by x-ray powder diffraction on crushed single crystalline samples. The analysis confirmed the single phase composition and the absence of foreign phases. The x-ray data were analyzed by standard Rietveld refinement using FULLPROF program [26]. For the crystallographic structure, the following parameters have been refined: the lattice parameter $a_0 = 10.246$ Å, the sulfur positional parameter $x = 0.266$ f.c., the three isotropic temperature factors, $B_{\text{iso}} = (1.16/1.35/2.31)$, for Hg, Cr, and S atoms, respectively. R_{Bragg} is 3.9 %.

The magnetization measurements were done utilizing a commercial SQUID magnetometer MPMS-5 (Quantum Design) in fields up to 5 T. The ultrasound-velocity and attenuation experiments were performed in the temperature range 2–300 K in static magnetic fields up to 14 T using a phase-sensitive setup [27].

The temperature dependences of the relative change of the sound velocity, $\Delta v/v$, (frame a) and sound attenuation (frame b) in HgCr_2S_4 are presented in Fig. 1 for different magnetic fields applied along the $\langle 111 \rangle$ axis. On decreasing temperature below 100 K in zero magnetic field, the sound velocity shows a continuous increase indicating a growing stiffness due to anharmonic effects as usually observed in solids. At 24 K the sound velocity exhibits a step-like upturn on approaching the magnetically ordered state followed by a more smooth growth on further decreasing temperature. The observed significant value of the additional upturn in $\Delta v/v$ of about 0.3 % on entering the AFM state indicates a strong magnetoelastic coupling. The transition into the long-range AFM state is accompanied by a sharp anomaly in the sound attenuation α (Fig. 1(b)) as well. Under the application of a magnetic field of 0.3 T the temperature dependence of the sound velocity becomes nonmonotonic. The anomaly in $\Delta v/v$ at T_N is transformed into a deep minimum that strongly shifts to lower temperatures reflecting the respective suppression of the transition temperature. The sharp anomaly in the sound attenuation is also strongly displaced to lower temperatures under the application of magnetic fields in correlation with ultrasound velocity data. Beside the sharp anomalies at T_N both quantities, $\Delta v/v$ and α , develop an additional broad anomaly which is shifted to higher temperatures with increasing magnetic fields. In the fields above 1 T the temperature

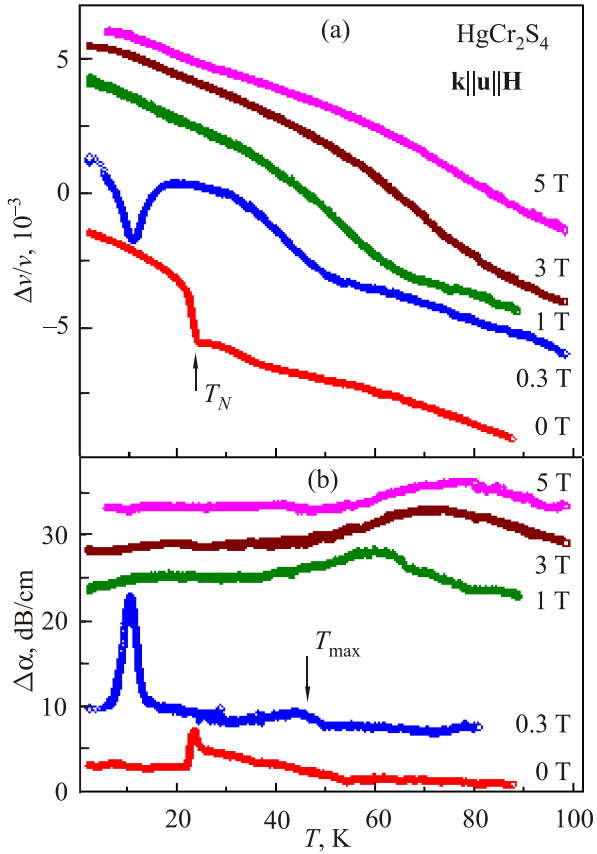


Fig. 1. Temperature dependences of the relative change of the sound velocity, $\Delta v/v$, (a) and sound attenuation (b) for HgCr_2S_4 single crystal measured in different magnetic fields applied along the $\langle 111 \rangle$ axis. The vertical arrows mark the magnetic phase transition at T_N in zero field and the anomaly at T_{\max} . The ultrasound frequency was set to 62 MHz. Here, \mathbf{k} is the wave vector and \mathbf{u} is the polarization of the longitudinal sound wave.

dependence of the sound velocity retains its monotonic character showing only continuous increase on decreasing temperatures.

In Fig. 2 the temperature dependences of the magnetization and derivative of the magnetization measured in different magnetic fields are shown. In the lowest field (0.01 T) the magnetization exhibits nonmonotonic temperature dependence with a strong increase of the magnetization below 70 K followed by a broad maximum at 30 K and a significant decrease at lower temperatures on entering the long-range AFM ordered state. The transition temperature $T_N = 23$ K corresponds to the maximum of the derivative of the magnetization, showing a sharp anomaly at this temperature. With increasing fields this anomaly is shifted to lower temperatures in correlation with the ultrasound data. In magnetic fields above 1 T the temperature dependence of the magnetization shows only monotonous increase on decreasing temperatures indicating induced ferromagnetic state. Beside the sharp anomaly at T_N another broad anomaly develops in the magnetization at high

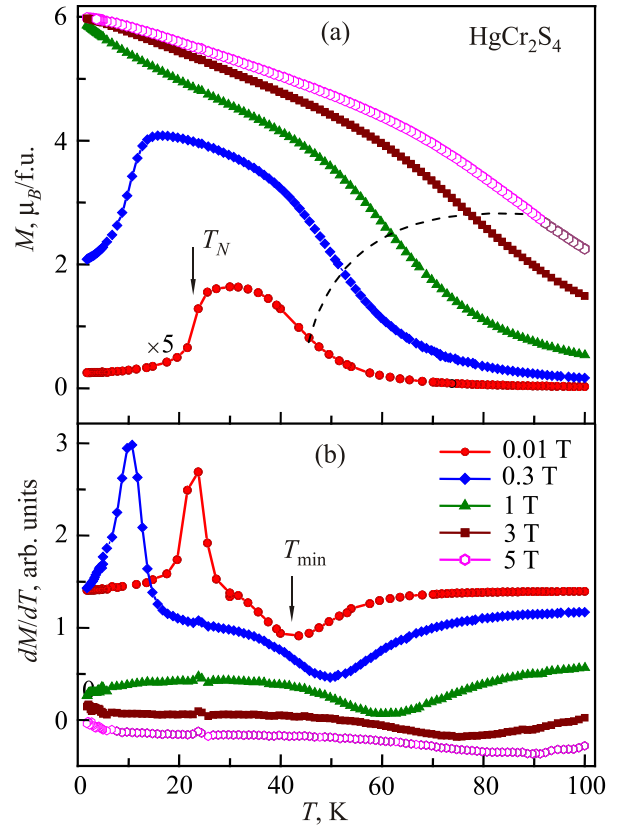


Fig. 2. Temperature dependences of the magnetization (a) and of the derivative of the magnetization (b) for HgCr_2S_4 single crystal measured in different magnetic fields applied along the $\langle 111 \rangle$ axis. The vertical arrows mark the magnetic phase transition at T_N in zero field and the anomaly at T_{\min} . Dashed line is guide to eye.

temperatures. It corresponds to a minimum in the derivative of the magnetization at T_{\min} which shifts to higher temperatures with increasing magnetic fields. We assume that at T_{\min} a balance of the competing ferromagnetic and antiferromagnetic interactions takes place. The increase of T_{\min} with temperature on increasing magnetic field might be explained by an increase of the FM correlations. We must additionally notice that the observed considerable increase of the magnetization in HgCr_2S_4 under the application of moderate magnetic field is unique among the chromium sulfide spinels.

To get further insight into the evolution of the AFM state with magnetic fields we studied the field dependences of the ultrasound and magnetization. The relative change of the sound velocity, $\Delta v/v$, at several temperatures measured in static magnetic fields is presented in Fig. 3. The data are shown for increasing and decreasing fields. At 2 K the acoustic mode shows an initial softening with increasing magnetic field. At a field of 0.6 T, $\Delta v/v$ reaches a minimum followed by an increase with further increasing field. This anomaly (minimum in $\Delta v/v$) manifests a pronounced hysteresis for field sweeps up and down indicating proba-

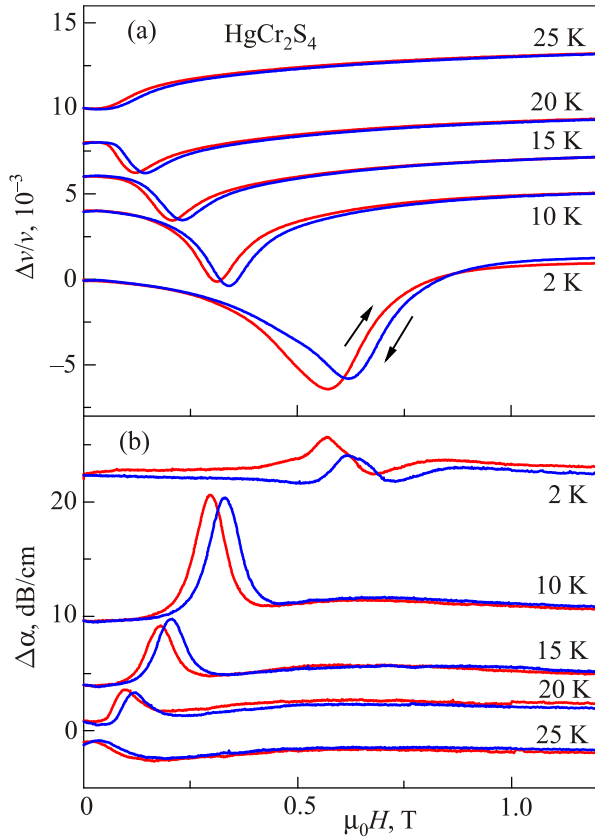


Fig. 3. Relative change of the sound velocity, $\Delta v/v$, (a) and attenuation α (b) vs magnetic field at different temperatures in HgCr_2S_4 . The ultrasound frequency was set to 48.4 MHz. The experimental geometry is the same as in Fig. 1.

bly irreversible transformation of the helical structure by magnetic fields. With increasing temperature within the magnetically ordered phase this anomaly shows a strong shift to lower fields and fully disappears for temperatures above 23 K. The ultrasound attenuation exhibits here a maximum that correlates with the respective anomaly in the sound velocity and experiences the similar evolution with temperature.

In Fig. 4 the field dependences of the magnetization and its derivative for different temperatures are presented. At 2 K, the magnetization curve $M(H)$ is strongly nonlinear showing a maximal slope between 0.3 and 0.5 T. With increasing temperature to 20 K, the initial slope of the $M = f(H)$ curve increases, but at temperatures above 25 K it decreases again (Fig. 4(b)). However, even at 40 K, $M(H)$ curve is still nonlinear as expected for induced ferromagnetic state.

The anomalies observed in the temperature and field dependences of the acoustic properties and magnetizations marks the phase boundaries which are plotted in the H - T phase diagram (Fig. 5). At temperatures below 23 K a long-range ordered antiferromagnetic state is established in zero field. The AFM state is continuously suppressed under the application of a magnetic field as reflected by a shift to lower temperatures of the anomalies in the acoustic pro-

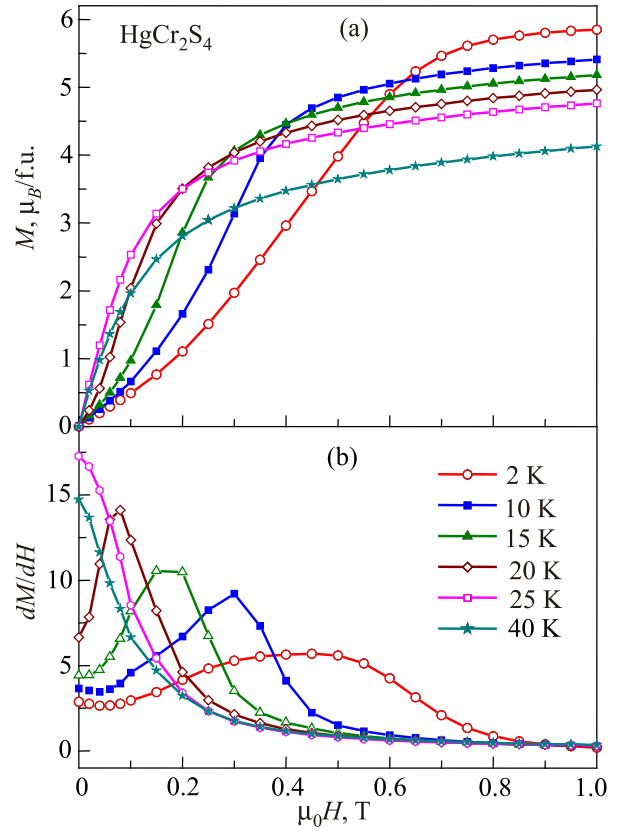


Fig. 4. Magnetization (a) and derivative of the magnetization (b) vs field for HgCr_2S_4 single crystals. Magnetic field is applied along the $\langle 111 \rangle$ axis.

perties and magnetization. In the fields above 1 T the AFM state is fully suppressed and an induced ferromagnetic (IFM) state is formed. Above 40 K, the broad anomalies that develop in the sound velocity, attenuation, and magnetization

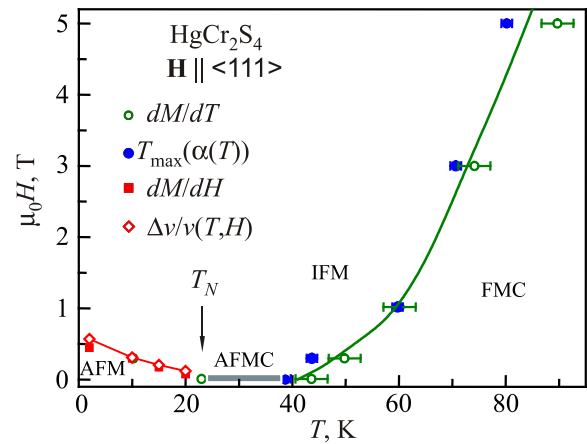


Fig. 5. (Color online) H - T phase diagram of HgCr_2S_4 spinel. The vertical arrow marks the transition into the long-range ordered AFM state. IFM denotes induced FM state; FMC is the state with dominating short-range ferromagnetic correlations; AFMC is the regime with dominating short-range antiferromagnetic correlations. The solid lines are guide to eye.

mark the high-temperature H - T phase boundary that separates the induced FM state and the disordered magnetic state with short-range FM correlations. This state is clearly different from the true paramagnetic state which is established only at much higher temperatures of ~ 250 K, as can be concluded from the deviation of the magnetic susceptibility from the Curie–Weiss law [24]. In between 23 and 40 K a narrow region (colored by grey) marks the regime with the antiferromagnetic short range correlations.

In conclusion, our detailed ultrasound propagation and magnetization studies of HgCr_2S_4 single crystals have revealed significant anomalies in the ultrasound velocity and attenuation at the magnetic transition into the spin-spiral AFM state indicating strong magnetoelastic coupling in this material. The observed evolution of the ultrasound velocity with temperature and magnetic field resembles the respective variation of the magnetization. Magnetic field strongly enhances the ferromagnetic correlations and suppresses the antiferromagnetic state. The nonmonotonic behavior of the magnetization and sound velocity disappears in magnetic fields above 1 T corresponding to the induced ferromagnetic state. The revealed strong magnetoelastic coupling in bond frustrated HgCr_2S_4 spinel must be taken into consideration in understanding the origin of the colossal magnetocapacitive effect and relaxor multiferroic behavior observed in this compound.

Acknowledgments

We acknowledge financial support via the institutional project 15.817.02.06F and projects for young researchers 15.819.02.01F. This work was partially supported by DFG via SFB 1143 and via the collaborative research center TRR 80 “From Electronic Correlations to Functionality” (Augsburg, Munich, and Stuttgart). We acknowledge the support of the HLD at HZDR, a member of the European Magnetic Field Laboratory (EMFL).

1. P.K. Baltzer, P.J. Wojtowicz, M. Robbins, and E. Lopatin, *Phys. Rev.* **151**, 367 (1966).
2. V. Tsurkan, H.-A. Krug von Nidda, A. Krimmel, P. Lunkenheimer, J. Hemberger, T. Rudolf, and A. Loidl, *Phys. Status Solidi A* **206**, 1082 (2009).
3. S.-H. Lee, C. Broholm, W. Ratcliff, G. Gasparovic, Q. Huang, T.H. Kim, and S.-W. Cheong, *Nature* **418**, 856 (2002).
4. J. Hemberger, P. Lunkenheimer, R. Ficht, H.-A. Krug von Nidda, V. Tsurkan, and A. Loidl, *Nature* **434**, 364 (2005).
5. A.P. Ramirez, R.J. Cava, and J. Krajewski, *Nature* **386**, 156 (1997).
6. V. Fritsch, J. Deisenhofer, R. Fichtl, J. Hemberger, H.-A. Krug von Nidda, M. Mucksch, M. Nicklas, D. Samusi, J.D. Thompson, R. Tidecks, V. Tsurkan, and A. Loidl, *Phys. Rev. B* **67**, 144419 (2003).
7. A.P. Ramirez, in *Handbook of Magnetic Materials*, K.H.J. Buschow (ed.), Elsevier Science, New York/North-Holland, Amsterdam (2001), Vol. 13, p. 423.
8. T. Rudolf, Ch. Kant, F. Mayr, J. Hemberger, V. Tsurkan, and A. Loidl, *New J. Phys.* **9**, 76 (2007).
9. Y. Yamashita and K. Ueda, *Phys. Rev. Lett.* **85**, 4960 (2000).
10. O. Tchernyshyov, R. Moessner, and S.L. Sondhi, *Phys. Rev. Lett.* **88**, 067203 (2002).
11. J. Hemberger, T. Rudolf, H.-A. Krug von Nidda, F. Mayr, A. Pimenov, V. Tsurkan, and A. Loidl, *Phys. Rev. Lett.* **97**, 087204 (2006).
12. J. Hemberger, H.A. Krug von Nidda, V. Tsurkan, and A. Loidl, *Phys. Rev. Lett.* **98**, 147203 (2007).
13. T. Rudolf, C. Kant, F. Mayr, J. Hemberger, V. Tsurkan, and A. Loidl, *Phys. Rev. B* **75**, 052410 (2007).
14. T. Rudolf, Ch. Kant, F. Mayr, J. Hemberger, V. Tsurkan, and A. Loidl, *Phys. Rev. B* **76**, 174307 (2007).
15. S. Weber, P. Lunkenheimer, R. Fichtl, J. Hemberger, V. Tsurkan, and A. Loidl, *Phys. Rev. Lett.* **96**, 157202 (2006).
16. M. Fiebig, *J. Phys. D* **38**, R123 (2005).
17. S.-W. Cheong and M. Mostovoy, *Nat. Mater.* **6**, 13(2007).
18. R. Ramesh and N.A. Spaldin, *Nat. Mater.* **6**, 21 (2007).
19. Y. Tokura and S. Seki, *Adv. Mater.* **22**, 1554 (2010).
20. B. Lüthi, *Physical Acoustics in the Solid State*, Berlin: Springer (2005).
21. P.K. Baltzer, P.J. Wojtowicz, M. Robbins, and E. Lopatin, *Phys. Rev.* **151**, 367 (1966).
22. J.M. Hasting and L.M. Corliss, *J. Phys. Chem. Solids* **29**, 9 (1968).
23. H.W. Lehmann and G. Harbeke, *Phys. Rev. B* **1**, 319 (1970).
24. V. Tsurkan, J. Hemberger, A. Krimmel, H.-A. Krug von Nidda, P. Lunkenheimer, S. Weber, V. Zestrea, and A. Loidl, *Phys. Rev. B* **73**, 224442 (2006).
25. L.C. Chapon, P.G. Radaelli, Y.S. Hor, M.T.F. Telling, and J.F. Mitchell, *ArXiv: cond-mat/060803* (2006), unpublished.
26. J. Rodriguez-Carvajal, *Physica B* **192**, 55 (1993).
27. S. Zherlitsyn, S. Yasin, J. Wosnitza, A.A. Zvyagin, A.V. Andreev, and V. Tsurkan, *Fiz. Nizk. Temp.* **40**, 160 (2014) [*Low Temp. Phys.* **40**, 123 (2014)].